Metformin Augments Anti-Inflammatory and Chondroprotective Properties of Mesenchymal Stem Cells in Experimental Osteoarthritis

Min-Jung Park,*[,1] Su-Jin Moon,[†,1] Jin-Ah Baek,* Eun-Jung Lee,* Kyung-Ah Jung,* Eun-Kyung Kim,* Da-Som Kim,* Jung-Ho Lee,[‡] Seung-Ki Kwok,[§] Jun-Ki Min,[¶] Seok Jung Kim,[‖] Sung-Hwan Park,[§,2] and Mi-La Cho*[,2]

Mesenchymal stem cells (MSCs) can protect against cartilage breakdown in osteoarthritis (OA) via their immunomodulatory capacities. However, the optimization strategy for using MSCs remains challenging. This study's objective was to identify the in vivo effects of metformin-stimulated adipose tissue-derived human MSCs (Ad-hMSCs) in OA. An animal model of OA was established by intra-articular injection of monosodium iodoacetate into rats. OA rats were divided into a control group and two therapy groups (treated with Ad-hMSCs or metformin-stimulated Ad-hMSCs). Limb nociception was assessed by measuring the paw withdrawal latency and threshold. Our data show that metformin increased IL-10 and IDO expression in Ad-hMSCs and decreased high-mobility group box 1 protein, IL-1β, and IL-6 expression. Metformin increased the migration capacity of Ad-hMSCs with upregulation of chemokine expression. In cocultures, metformin-stimulated Ad-hMSCs inhibited the mRNA expression of RUNX2, COL X, VEGF, MMP1, MMP3, and MMP13 in IL-1β–stimulated OA chondrocytes and increased the expression of TIMP1 and TIMP3. The antinociceptive activity and chondroprotective effects were greater in OA rats treated with metformin-stimulated Ad-hMSCs than in those treated with unstimulated Ad-hMSCs. TGF-β expression in subchondral bone of OA joints was attenuated more in OA rats treated with metformin-stimulated Ad-hMSCs. Our findings suggest that metformin offers a promising option for the clinical application of Ad-hMSCs as a cell therapy for OA. ***The Journal of Immunology*****, 2019, 203: 127–136.**

Osteoarthritis (OA) is the most common degenerative joint disease that gradually wears articular cartilage, subsequent joint space narrowing, changes in subchondral bone, and chronic pain. Chondrocytes are the only cells that present in articular cartilage. Various factors, including age, obesity, trauma history, muscle weakness, and genetics predisposition can affect both the onset and progression of OA (1). However, the fact that an imbalance between catabolic (inflammatory) and anabolic activities of articular chondrocytes leads to the occurrence of the disease is important in an attempt to control OA development. Studies of cartilage biology have provided insights into chondrocyte apoptosis as a key player in cartilage degeneration in OA (2–4).

Accumulating evidence indicates that low-grade inflammation plays a critical role in the development and progression of OA (5). In the past decades, there has been a fundamental shift in understanding of the mechanisms underlying OA. The disease is no longer considered to be a natural phenomenon of normal body wear and tear but rather a disorder caused by chronic, low-grade inflammation (5). Although the extent and features of OA inflammation differ from those of rheumatoid arthritis, proinflammatory cytokines, chemokines, and growth factors, such as MCP-1, IL-1β, and IL-6, have been identified as factors that mediate the disturbed homeostasis in the OA cartilage matrix (6–9). Among them, IL-1β, a representative proinflammatory cytokine, is involved in OA pathogenesis via increased cartilage catabolism and concomitant increases in cartilage anabolism and repair (10).

Mesenchymal stem cells (MSCs) are present in various human tissues, including bone marrow, peripheral blood, cord blood, and adipose tissue (11–14). These multipotent stem cells have the capacity

*The Rheumatism Research Center, Catholic Research Institute of Medical Science, The Catholic University of Korea, Seoul 137-701, South Korea; [†]Division of Rheumatology, Department of Internal Medicine, Uijeongbu St. Mary's Hospital, College of Medicine, The Catholic University of Korea, Seoul 137-701, South Korea; [‡]Department of Plastic and Reconstructive Surgery, Bucheon St. Mary's Hospital, College of Medicine, The Catholic University of Korea, Seoul 137-701, Korea; [§]Division of Rheumatology, Department of Internal Medicine, Seoul St. Mary's Hospital, College of Medicine, The Catholic University of Korea, Seoul 137-701, South Korea; [¶]Division of Rheumatology, Department of Internal Medicine, Bucheon St. Mary's Hospital, College of Medicine, The Catholic University of Korea, Seoul 137-701, South Korea; and [‖]Department of Orthopedic Surgery, Uijeongbu St. Mary's Hospital, College of Medicine, The Catholic University of Korea, Seoul 137-701, Korea

[1]M.-J.P. and S.-J.M. contributed equally to this work.

[2]S.-H.P. and M.-L.C. contributed equally to this work.

ORCIDs: 0000-0002-9116-8786 (S.J.K.); 0000-0003-1711-2060 (S.-H.P.).

Received for publication January 4, 2018. Accepted for publication May 1, 2019.

This work was supported by a grant of the Korea Health Technology Research and Development Project through the Korea Health Industry Development Institute, funded by the Ministry of Health and Welfare, Republic of Korea (HI15C1062 and HI16C1888), and by the Bio and Medical Technology Development Program of the National Research Foundation, funded by the Korean government (Ministry of Science and ICT) (NRF-2017M3A9B4028022).

Address correspondence and reprint requests to Dr. Sung-Hwan Park, Division of Rheumatology, Department of Internal Medicine, School of Medicine, The Catholic University of Korea, Seoul St. Mary's Hospital, 505 Banpo-dong, Seocho-gu, Seoul 137-701, South Korea or Dr. Mi-La Cho at the current address: Department of Biomedicine & Health Sciences, College of Medicine, The Catholic University of Korea, 222 Banpo-daero, Seocho-gu, Seoul 06591, South Korea. E-mail addresses: rapark@catholic.ac.kr (S.-H.P.) or iammila@catholic.ac.kr (M.-L.C.)

The online version of this article contains supplemental material.

Abbreviations used in this article: Ad-hMSC, adipose tissue-derived human MSC; CGRP, calcitonin gene-related peptide; COL X, type X collagen; DRG, dorsal root ganglion; HMGB1, high mobility group box 1; MIA, monosodium iodoacetate; MSC, mesenchymal stem cell; OA, osteoarthritis; PWL, paw withdrawal latency; PWT, paw withdrawal threshold; RUNX2, runt-related transcription factor-2; TEM, transmission electron microscopy; VEGF, vascular endothelial growth factor.

to differentiate into mesodermal lineages such as osteoblasts, chondrocytes, and adipocytes. MSCs have been suggested to play an intrinsic role in tissue repair and regeneration and to have anti-inflammatory activities. Based on the evidence of their pluripotent differentiation and immunomodulatory properties, MSCs have been at the center of attention in the field of regenerative medicine, especially with regard to OA. MSCs secrete various growth factors and cytokines that are inferred actors in OA progression, such as vascular endothelial growth factor (VEGF) (15), and IL-6 (16), which makes them targets for intervention. It is believed that some growth factors or inflammatory cytokines secreted by MSCs might hamper the therapeutic potential of these cells, in particular their ability to inhibit the development and progression of OA.

Metformin, a first-line antidiabetic agent, has anti-inflammatory and antioxidant effects (17). Recent studies have revealed the autophagy inducing property of metformin (18). Interestingly, autophagy induction in MSCs can enhance cell survival (19). In the current study, we showed that metformin treatment in adipose tissue-derived human MSCs (Ad-hMSCs) can enhance their immunomodulatory properties and migration capacity. In a rat model of OA, metformin-treated Ad-hMSCs showed potent inhibition of cartilage degeneration and antinociceptive properties, and these changes were associated with attenuated expression of TGF-β in subchondral bone. Our findings suggest a potential role of metformin treatment as a revolutionary strategy to optimize the possibility of the Ad-hMSCs as a cell therapy in OA.

Materials and Methods

Mice

Six-week-old male Wistar rats weighing 140–230 g at the start of the experiment were purchased from Central Lab Animal (Seoul, South Korea). The animals were housed three per cage in a room with controlled temperature conditions (21–22˚C) and lighting (12 h light/dark cycle), with access to sterile food and water. All experimental procedures were examined and approved by the Animal Research Ethics Committee of The Catholic University of Korea (2016-0255-01), in conformity with the National Institutes of Health guidelines.

Isolation and culture of Ad-hMSCs

Liposuction of s.c. fat was carried out in patients under general anesthesia by an experienced surgeon. Lipoaspirates were collected from five volunteers, and adipose tissue was digested with RTase (4 ml/g fat; Biostar Stem Cell Research Institute, Nature Cell, Seoul, Korea) for 60 min at 37˚C. The digested tissues were filtered through a 100-μm nylon sieve to remove cellular debris and then centrifuged at 470 × *g* for 5 min. The pellet obtained was resuspended in RCME cell attachment medium (Nature Cell) and cultured overnight at 37˚C in a humidified atmosphere with 5% CO_2. After 24 h, the cultures were washed with PBS to remove nonadherent cells. The medium was changed to RKCM cell growth medium (Nature Cell) containing 5% FBS (Invitrogen, Carlsbad, CA). The cells were cultured for 4 d until 90% confluent (passage 0) and were then expanded for two to three passages and used for experiments. Ad-hMSCs were stimulated with metformin (1 mM) for 48 h. A schematic presentation of metformin treatment in Ad-hMSCs is illustrated in Supplemental Fig. 1.

Induction of OA and treatment with metformin-stimulated Ad-hMSCs

Animals were randomly assigned to treatment groups before the study began. After anesthetization with isoflurane, rats were injected with 3 mg of monosodium iodoacetate (MIA) (Sigma-Aldrich, St. Louis, MO) in a 50-μl volume using a 26.5-G needle inserted through the patellar ligament into the intra-articular space of the right knee; control rats were injected with an equivalent volume of saline. MSCs or metformin-stimulated MSCs were injected i.v. in the MIA-treated rats.

Assessment of pain behavior

MIA-treated rats were randomized to experimental groups. Nociception was tested using a dynamic plantar esthesiometer (Ugo Basile, Gemonio, Italy), an automated version of the von Frey hair assessment procedure, before MIA injection (day 0), and was measured once every 3 d thereafter. The rats were placed on a metal mesh surface in an acrylic chamber in a temperature-controlled room (21–22˚C) and rested for 15 min before testing. The touch stimulator unit was oriented beneath the animal, and an adjustable angled mirror was used to place the stimulating microfilament (0.5-mm diameter) below the plantar surface of the hind paw. When the instrument was activated, a fine plastic monofilament advanced at a constant speed and touched the paw in the proximal metatarsal region. The filament exerted a gradually increasing force on the plantar surface, starting below the threshold of detection and increasing until the stimulus became painful, as indicated by removal of the paw. The force required to elicit a paw withdrawal reflex was recorded automatically and measured in grams. A maximum force of 50 g and a ramp speed of 20 s were used for all esthesiometry tests. Pain behavioral tests of secondary tactile allodynia were conducted immediately before injection of MSCs or metformin-stimulated MSCs.

Real-time PCR

The mRNA expression levels were estimated using a LightCycler 2.0 instrument (Roche Diagnostic, Mannheim, Germany) with version 4.0 software. All reactions were performed with LightCycler FastStart DNA Master SYBR Green I (Takara, Shiga, Japan) following the manufacturer's instructions. Relative mRNA levels were normalized to that of β-actin. Primers were used to amplify the following genes: high mobility group box 1 (HMGB1), IL-1β, IL-6, IDO, IL-10, CCR1, CCR3, CCR4, CXCR4, CCR7, runt-related transcription factor-2 (RUNX2), type X collagen (COL X), VEGF, MMP13, MMP1, MMP3, TIMP1, TIMP3, and β-actin (Table I).

Table I. Primers used in the PCRs

Gene	Forward	Reverse
HMGB1	5′-GATCCCAATGCACCCAAGAG-3′	5′-TTCGCAACATCACCAATGA-3′
IL-1β	5′-GGACAAGCTGAGGAAGATGC-3′	5′-TCGTTATCCCATGTGTCGAA-3′
IL-6	5′-AATTCGGTACATCCTCGCGG-3′	5′-GGTTGTTTTCTGCCAGTGCC-3′
IDO	5′-TTTGGGTCTTCCCAGAACC-3′	5′-GCGCTGTTGGAAATAGCTTC-3′
IL-10	5′-CCAAGCCTTGTCTGAGATGA-3′	5′-TGAGGGTCTTCAGGTTCTCC-3′
CCR1	5′-ACCATAGGAGGCCAACCCAAAATA-3′	5′-TCCATGCTGTGCCAAGAGTCA-3′
CCR3	5′-TTTGTCATCATGGCGGTGTTTTTC-3′	5′-GGTTCATGCAGCAGTGGGAGTAG-3′
CCR4	5′-GAGAAGAAGAACAAGGCGGTGAAGA-3′	5′-GGATTAAGGCAGCAGTGAACAAAAG-3′
CCR7	5′-GCCGAGACCACCACCACCTT-3′	5′-AGTCATTGCATCTGCTCCCTATCC-3′
CXCR4	5′-ATCCCTGCCCTCCTGCTGACTATTC-3′	5′-GAGGGCCTTGCGCTTCTGGTG-3′
RUNX2	5′-CTGAGATTTGTGGGCCGGA-3′	5′-GGGGAGGATTTGTGAAGACGG-3′
COL X	5′-ACAGGAATGCCTGTGTCTGCTTTACT-3′	5′-CATTGGGAAGCTGGAGCCACACCTGGTC-3′
VEGF	5′-CCATGAACTTTCTGCTGTCTT-3′	5′-ATCGCATCAGGGGCACACAG-3′
MMP13	5′-CTATGGTCCAGGAGATGAAG-3′	5′-AGAGTCTTGCCTGTATCCTC-3′
MMP1	5′-CTGAAGGTGATGAAGCAGCC-3′	5′-AGTCCAAGAGAATGGCCGAG-3′
MMP3	5′-CTCACAGACCTGACTCGGTT-3′	5′-CACGCCTGAAGGAAGAGATG-3′
TIMP1	5′-AATTCCGACCTCGTCATCAG-3′	5′-TGCAGTTTTCCAGCAATGAG-3′
TIMP3	5′-CTGACAGGTCGCGTCTATGA-3′	5′-GGCGTAGTGTTTGGACTGGT-3′
β-actin	5′-GGACTTCGAGCAAGAGATGG-3′	5′-TGTGTTGGGGTACAGGTCTTTG-3′

Western blotting

Proteins were separated by $NaDodSO_4$ PAGE (SDS-PAGE) and transferred to nitrocellulose membranes (Amersham Pharmacia Biotech, Buckinghamshire, U.K.). Membranes were stained with primary Abs against MMP1, MMP13, COL X, VEGF, TIMP1, TIMP3, GAPDH (all from Cell Signaling Technology, Danvers, MA), and β-actin. An HRP-conjugated secondary Ab was then added.

Confocal microscopic analysis

Ganglion was snap frozen in liquid nitrogen and stored at 80°C. Tissue sections (7 μm) were fixed in methanol and acetone, blocked with 10% goat serum, and stained with anti–calcitonin gene-related peptide (CGRP) (Abcam) and anti-rabbit IgG-PE secondary Ab (SouthernBiotech). The nuclei were stained with DAPI. The stained sections were analyzed using a Zeiss microscope (LSM 510 Meta; Carl Zeiss, Oberkochen, Germany) at 400× magnification.

Transmission electron microscopy

The cells were harvested, centrifuged (215 × *g* for 10 min), washed with cold PBS, and fixed with 2.5% glutaraldehyde (in 0.2 M sodium cacodylate, pH 7.4). The samples were then fixed in 1% OsO_4 for 1 h at 4°C, dehydrated with increasing concentrations of ethanol, embedded in Spurr resin, and sectioned. Ultrathin sections were cut, stained with uranyl acetate, and observed by transmission electron microscopy (TEM).

ELISA

The concentrations of IL-10 (ABNOVA, Tappei, Taiwan) in culture supernatants and serum samples were measured using a sandwich ELISA (DuoSet; R&D Systems, Lille, France).

Flow cytometry analysis

mAbs conjugated to fluorescent dyes targeting human CD13, CD90, CD105, CD29, CD44, CD11b, CD19, CD31, CD34, CD45, and HLA-DR (BD Biosciences, Schwechat, Austria) were used to characterize the MSCs. Their surfaces were stained using different combinations of the following mAbs (all from Pharmingen, San Diego, CA, unless indicated): CD13–PE (L138, IgG_1, κ); CD90–PE (5E10, IgG1, κ); CD11b–PE (ICRF44, IgG_1, κ); CD19–PE (HIB19, IgG1, κ); CD34–PE (8G12, IgG1, κ); CD34–FITC (MMA, IgM); CD105–allophycocyanin (RPA-T4, IgG1; BioLegend, San Diego, CA); CD29–PE (RPA-T8, IgG1, κ); CD44–FITC (HI100, IgG2b, κ); CD45–allophycocyanin (M-A251, IgG1, κ); and HLA-DR–PE (G46-6, IgG2a, κ). The data were analyzed using the FlowJo software (Tree Star, Ashland, OR).

Transwell migration assay

Migration assays were performed in a 24-well Transwell unit with 8-μm pores (Corning Costar, Cambridge, MA). MSCs or metformin-stimulated MSCs were seeded at a density of 6×10^5 cells/ml in 100 μl of medium (α-minimal essential medium + 1% FBS) in the upper chamber of the Transwell assembly. The lower chamber contained 600 μl of medium with 30 ng/ml stromal-derived factor-1 (PeproTech, Rocky Hill, NJ). After incubation at 37°C in 5% CO_2 for 10 h, the upper surface of the membrane was scraped gently to remove nonmigrating cells and washed with PBS. The membrane was then fixed in 4% paraformaldehyde for 15 min and stained with 0.5% crystal violet for 10 min.

Evaluation of MSC differentiation

Primary Ad-hMSCs were differentiated using a commercially available differentiation kit (R&D Systems). Briefly, the cells were plated in 24-well plates (for adipogenic and osteogenic differentiation) or 15-ml conical tubes (for chondrogenic differentiation) and cultured in each differentiation medium. After 1 wk (adipogenic differentiation) or 3 wk (osteoblastogenic and chondrogenic differentiation), cells were fixed and stained with DAPI and with Abs to fatty acid binding protein 4 (FABP-4), osteocalcin, and aggrecan and visualized by fluorescence microscopy.

Primary culture and treatment of OA chondrocytes

The study was approved by the local ethics committee, and informed consent was obtained from all patients with OA, who fulfilled the American College of Rheumatology criteria for this disease (20). Human chondrocytes were isolated from OA patients as described previously (21). Chondrocytes (1×10^5 cells per well) were placed in 24-well tissue culture plates, and the medium was replaced with serum-free DMEM the following day. The chondrocytes were stimulated with recombinant human IL-1β (20 ng/ml; R&D Systems) for 48 h. IL-1β–pretreated chondrocytes were cultured with or without Ad-hMSCs. Unstimulated Ad-hMSCs or metformin-stimulated Ad-hMSCs were resuspended at 5×10^5/ml in the appropriate medium supplemented with 1% FBS and seeded in the upper chamber. Our study was approved by the institutional review board of Bucheon St. Mary's Hospital and was performed in accordance with the Helsinki II Declaration. All patients were informed and gave their written consent.

Assessment of apoptosis

To quantify apoptosis, a TUNEL assay was performed according to the manufacturer's protocol (In Situ Cell Death Detection Kit, fluorescein; Roche Diagnostics). The apoptotic index is expressed as a percentage of the TUNEL-positive cells.

Histological and immunohistochemical analyses

A modified Mankin histological score was used to score histological injuries of the articular cartilage as follows. The structure was scored on a scale of 0–6, where 0 = normal; 1 = irregular surface, including fissures into the radial layer; 2 = pannus; 3 = absence of superficial cartilage layers; 4 = slight disorganization (cellular row absent, some small superficial clusters); 5 = fissure into the calcified cartilage layer; and 6 = disorganization (chaotic structure, clusters, and osteoclasts activity). Cellular abnormalities were scored on a scale of 0–3, where 0 = normal; 1 = hypercellularity, including small superficial clusters; 2 = clusters; and 3 = hypocellularity. The matrix staining was scored on a scale of 0–4, where 0 = normal/slight reduction in staining; 1 = staining reduced in the radial layer; 2 = staining reduced in the interterritorial matrix; 3 = staining present only in the pericellular matrix; and 4 = staining absent. Joint space width was estimated measuring the sum of the nearest distance of medial and lateral tibiofemoral joints. Histological evaluation was performed by two independent experienced researchers who were blinded to the treatment arm. Immunohistochemistry was performed using a VECTASTAIN ABC kit (Vector Laboratories, Burlingame, CA). Tissue sections were incubated overnight at 4°C with the primary Abs against TGFβ, followed by probing with a biotinylated secondary Ab and then streptavidin–peroxidase complex for 1 h. The final color product was developed using 3,3′-diaminobenzidine chromogen (Dako, Carpinteria, CA).

In vivo imaging analysis

To evaluate the effects of metformin treatment on homing of MSCs to inflamed joints, MSCs were stained with DiD fluorescent dye (Life Technologies, Molecular Probes) according to the manufacturer's instructions. MSCs or metformin-treated MSCs were injected i.v. 3 d after MIA injection and imaged by scanning in a prewarmed (37°C) IVIS Spectrum in vivo imaging system (PerkinElmer, MA). Data were analyzed using Living Image software (PerkinElmer) to evaluate the average signal intensity of regions of interest. The lowest signal was adjusted to the level of autofluorescence background.

Statistical analysis

Data are presented as mean ± SD of at least five independent experiments or at least three independent samples and for eight mice in each group. One-way ANOVA followed by Bonferroni post hoc test was used to compare differences between ≥3 groups. The Mann–Whitney *U* test was used to compare numerical data between two groups. To assess the Gaussian distribution and the equality of variance, Shapiro–Wilk test and Levene test were used, respectively. A p value <0.05 was considered statistically significant. Statistical analysis was performed using IBM SPSS Statistics 20 for Windows (IBM, Armonk, NY).

Results

Metformin-induced regulation of the immunoregulatory properties of Ad-hMSCs via autophagy induction and enhanced mitochondrial function

To assess whether metformin can regulate inflammatory molecules in Ad-hMSCs, the mRNA expression of inflammatory mediators, HMGB1, IL-1β, and IL-6 were analyzed by real-time PCR in Ad-hMSCs incubated with or without metformin. HMGB1 is an evolutionarily ancient nuclear protein that functions to initiate and perpetuate immune responses and to mediate inflammatory responses (22). We found significantly suppressed levels of HMGB1, IL-1β, and IL-6 mRNA in metformin-treated Ad-hMSCs compared

with untreated Ad-hMSCs (Fig. 1A). Next, to determine whether metformin treatment can influence the immunoregulatory activities in Ad-hMSCs, synthesis of IDO and IL-10 mRNA was analyzed by real-time PCR in Ad-hMSCs incubated with or without metformin. Metformin pretreatment increased IDO and IL-10 mRNA levels (Fig. 1B). The concentrations of HMGB-1, IL-1β, IL-6, and IL-10 in culture supernatants were increased by metformin treatment (Fig. 1C). Confocal microscopy using triple-immunofluorescence staining was used to compare IDO and IL-10 expression between untreated Ad-hMSCs and metformin-treated Ad-hMSCs. IDO and IL-10 expression was abundant in the metformin-treated Ad-hMSCs but was faint in the Ad-hMSCs not exposed to metformin (Fig. 1D).

Next, to determine how metformin affects the immunoregulatory properties of Ad-hMSCs, the cells were incubated with or without 1 mM metformin. Compared with untreated cells, metformin-treated cells showed the formation of small vacuoles inside the cells after 48 h incubation, which is consistent with its autophagy-inducing properties (Fig. 1E). TEM revealed that exposure of Ad-hMSCs to metformin resulted in the appearance of autophagic vacuoles (red arrows, Fig. 1E). And, metformin treatment in Ad-hMSCs increased mitochondrial cristae and density in the cells, whereas untreated Ad-hMSCs contained swollen and fewer mitochondria (yellow arras, Fig. 1E). These data suggest that metformin pretreatment stimulated the immunoregulatory properties of Ad-hMSCs and that this was associated with autophagy induction and improved mitochondrial function.

Increased migration capacity of metformin-treated Ad-hMSCs without effects on MSC characteristics

To determine whether metformin treatment in MSC can affect their surface phenotype, we compared and analyzed the expression of typical MSC surface marker profiles in metformin-treated Ad-hMSCs and untreated Ad-hMSCs by flowcytometry. Ad-hMSCs in both groups (with or without metformin) expressed the mesenchymal cell surface markers CD90, CD13, CD44, CD29, and CD105 and were negative for CD11b, CD19, CD31, CD34, CD45, and HLA-DR (Fig. 2A). Metformin treatment did not affect the surface Ag profiles.

To determine whether the cells were capable of differentiating into multiple cell lineages, Ad-hMSCs were cultured under different conditions: in adipogenic medium (Fig. 2B, upper panel), osteogenic medium (Fig. 2B, medium panel), or chondrogenic medium (Fig. 2B, lower panel). Metformin did not affect the differentiation capacities of Ad-hMSCs. Next, we studied the in vitro migration capacity of metformin-treated Ad-hMSCs. Ad-hMSCs

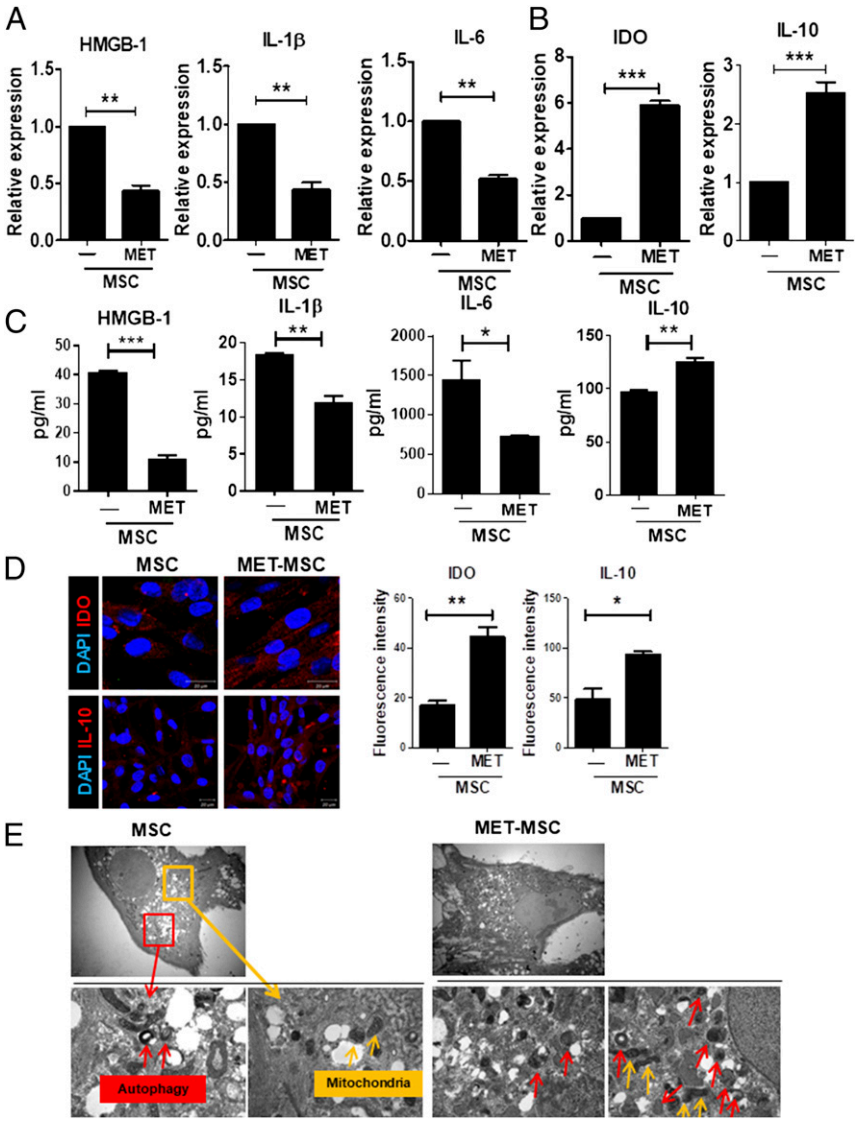

FIGURE 1. Immunoregulatory properties of Ad-hMSCs after metformin treatment. (**A**) Expression of HMGB-1, IL-1β, and IL-6 was analyzed by real-time PCR in Ad-hMSCs incubated with or without metformin. (**B**) Expression of IDO and IL-10 was analyzed by real-time PCR. (**C**) The concentrations of HMGB-1, IL-1β, IL-6, and IL-10 were analyzed by sandwich ELISA in Ad-hMSCs incubated with or without metformin (1 mM). (**D**) Immunofluorescence staining of cultured Ad-hMSCs treated with or without metformin (1 mM) with IL-10 (red) or IDO (red) and counterstained with DAPI (blue). Original magnification ×400. Data are presented as means ± SD and represent three independent experiments. $*p < 0.05$, $**p < 0.01$, $***p < 0.001$ versus untreated Ad-hMSCs. (**E**) TEM showed that Ad-hMSCs treated with metformin (1 mM) exhibited numerous cytoplasmic vacuoles, most of which were identified clearly as autophagosomes (with a visible double membrane; red arrows) and increased number of mitochondria (yellow arrows) compared with untreated Ad-hMSCs. Upper panel, Original magnification ×4000. Lower panel, Original magnification ×15,000. Data are representative of at least two independent experiments.

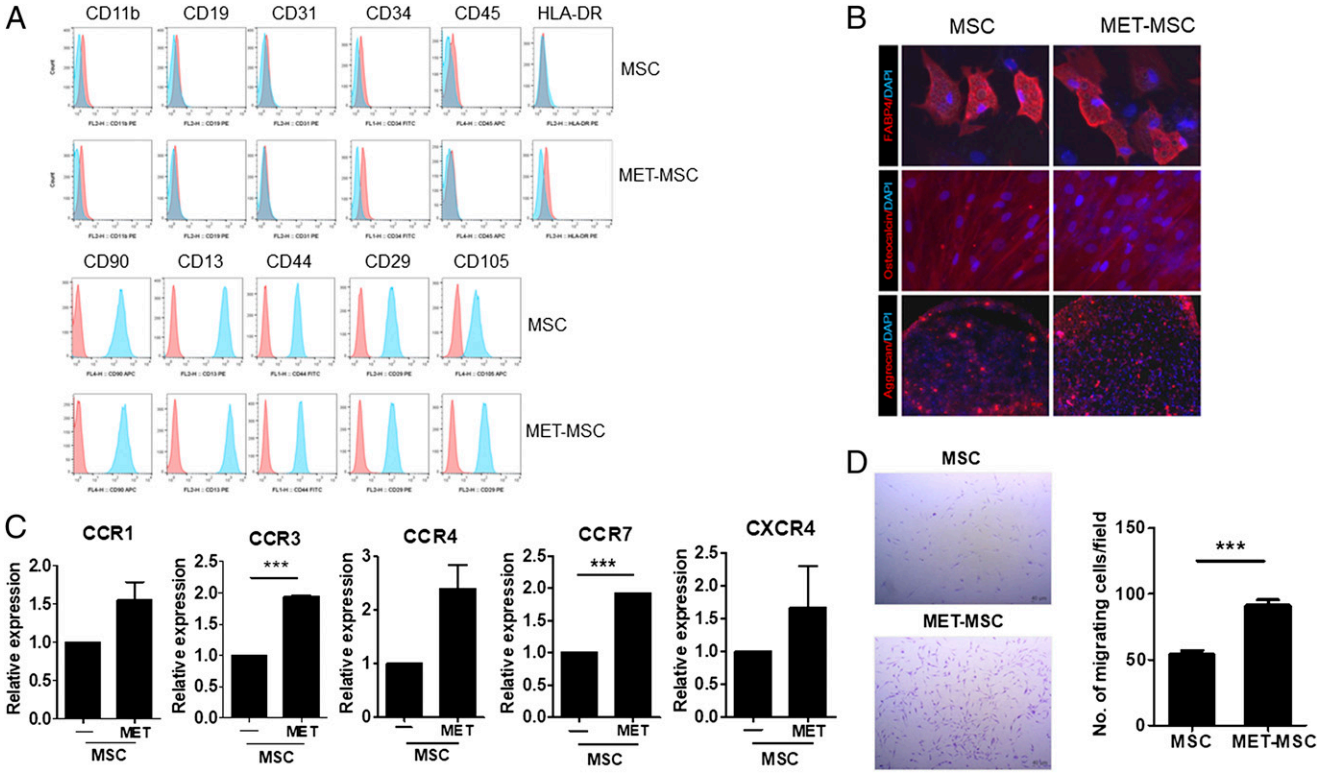

FIGURE 2. Characterization and in vitro migration capacity of Ad-hMSCs after metformin treatment. (**A**) Expression of markers in Ad-hMSCs was analyzed by flow cytometry. From left to right: (upper row) CD11b, CD19, CD31, CD34, CD45, HLA-DR and (lower row) CD90, CD13, CD44, CD29, CD105. Red histograms, cells stained with isotype control; blue histograms, cells isolated with specific Abs. Data are representative of at least two independent experiments. (**B**) Ad-MSCs were plated on each type of differentiation medium. After 1 (adipogenic differentiation) or 3 wk (osteoblastogenic and chondrogenic differentiation), cells were fixed and stained with Abs to FABP-4 (top), osteocalcin (middle), or aggrecan (bottom) and visualized by fluorescence microscopy. Original magnification ×400. Representative images into adipogenic, osteogenic, and chondrogenic pathways. (**C**) mRNA expression of chemokine receptors in Ad-hMSCs treated with or without metformin was assessed by real-time PCR. Graphs represent the mean chemokine receptor expression of Ad-hMSCs treated with metformin (1 mM) compared with the negative control (untreated Ad-hMSCs), and bars represent the SD from three independent experiments. (**D**) Migration assay of Ad-hMSCs in response to SDF-1 stimulation. Original magnification ×40. The bar graphs represent the numbers of migrating Ad-hMSCs expressed as means ± SD of three independent experiments. ***$p < 0.001$.

expressed CCR1, CCR3, CCR4, CCR7, and CXCR,4 which are involved in the migratory capacities of MSCs. The expression of CCR1, CCR3, CCR4, CCR7, and CXCR4 mRNA was significantly higher in metformin-treated Ad-hMSCs than in untreated Ad-hMSCs (Fig. 2C). Because migration of MSCs into injured tissues can directly affect their immunomodulating capacities in inflammatory milieu, we studied whether the migration capacity was enhanced by metformin treatment. The in vitro migration efficiency was significantly higher (1.7-fold increase) by metformin treatment, compared with the untreated cells (Fig. 2D). Overall, these results indicate that metformin treatment in Ad-hMSCs can enhance their migration capacity while preserving their MSC characteristics, such as surface Ag profiles and multilineage differentiation.

Recovery of anabolic and catabolic activities and decreased apoptosis of human OA chondrocytes cocultured with metformin-stimulated Ad-hMSCs

To evaluate whether metformin treatment of Ad-hMSCs affects inflammatory and catabolic processes in OA chondrocytes, IL-1β–stimulated OA chondrocytes were cocultured with unstimulated Ad-hMSCs or metformin-treated Ad-hMSCs (Fig. 3A). RUNX2, whose expression is increased in OA cartilage, is an early contributing factor to the development of OA via induction of chondrocyte hypertrophy (23). RUNX2 is associated with increased expression of MMP-13 and COL X, which causes cartilage degradation as part of the endochondral ossification process of growth plate development (24–26). Metformin treatment in Ad-hMSCs significantly blocked IL-1β–stimulated RUNX2, COL-X, VEGF, and MMP mRNA expression but induced TIMP1 and TIMP3 expression in OA chondrocytes cocultured with the cells (Fig. 3A). The Western blot showed the same results (Fig. 3B). The protein expressions of MMP1, MMP13, COL-X, and VEGF was attenuated in OA chondrocytes that were cocultured with metformin-treated Ad-hMSCs, whereas TIMP1 and TIMP3 expressions were significantly increased (Fig. 3B).

Chondrocytes are the only resident cell involved in the maintenance of the extracellular matrix in articular cartilage. Although it is not clear whether chondrocyte apoptosis directly induces OA progression or is a byproduct of cartilage destruction, apoptosis is clearly implicated in human OA. There is a significant correlation between the increasing numbers of chondrocyte apoptosis and severity of OA in both animal and human models (27–30). Therefore, we investigated whether metformin-stimulated Ad-hMSCs could inhibit chondrocyte apoptosis of human OA chondrocytes in coculture. A TUNEL assay was used to evaluate cell apoptosis. Apoptotic cells were observed in IL-1β–stimulated OA chondrocytes (Fig. 3C, left panel). Quantitative analysis of the TUNEL-positive chondrocytes showed that the number of apoptotic cells was significantly decreased when cocultured with Ad-hMSCs (Fig. 3C, middle

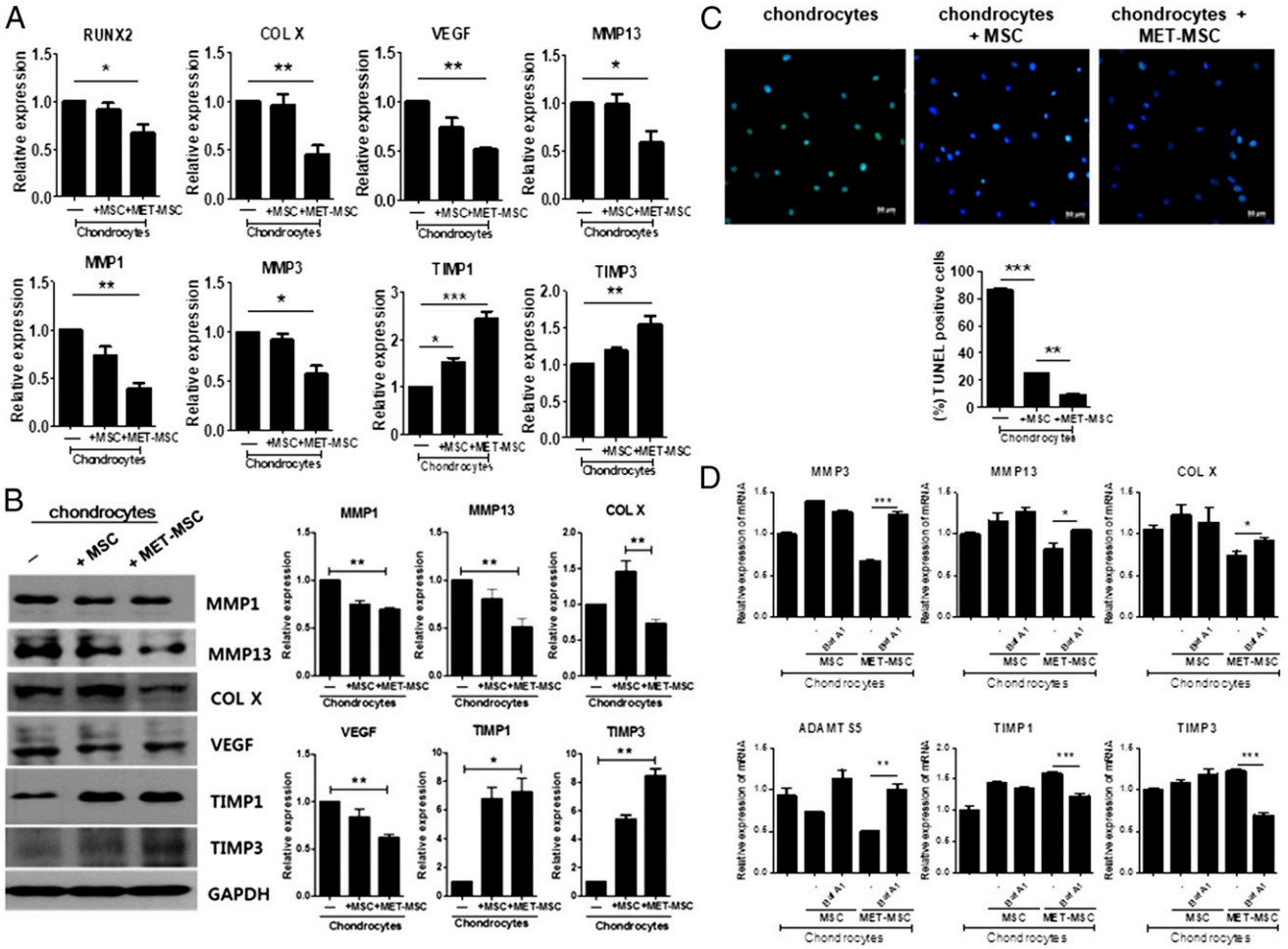

FIGURE 3. Effects of metformin-stimulated Ad-hMSCs on gene expression levels in IL-1β–stimulated OA chondrocytes. (**A** and **B**) mRNA (A) and protein expressions (B) of RUNX2, COL X, VEGF, MMP13, MMP1, MMP3, TIMP1, and TIMP3 in IL-1β–stimulated OA chondrocytes cocultured with or without unstimulated Ad-hMSCs or metformin-stimulated Ad-hMSCs were measured by quantitative real-time PCR and Western blot, respectively. β-actin and GAPDH were used as the internal control. (**C**) Detection of apoptosis of OA chondrocytes by the TUNEL assay. Original magnification ×400. The blue DAPI stain marks intact DNA (left panel). The apoptotic index of the groups (right panel). Coculture with metformin-stimulated Ad-hMSCs significantly inhibited the apoptosis of OA chondrocytes compared with unstimulated Ad-hMSCs. (**D**) mRNA expression of MMP3, MMP13, COL X, ADAMTS5, TIMP1, and TIMP3 in IL-1β–stimulated OA chondrocytes cocultured with unstimulated Ad-hMSCs or metformin-stimulated Ad-hMSCs in the presence or absence of bafilomycin A1 were measured by quantitative real-time PCR. $*p < 0.05$, $**p < 0.01$, $***p < 0.001$. BafA1, bafilomycin A1.

panel and bar graph). Interestingly, metformin-stimulated Ad-hMSCs inhibited the apoptosis of OA chondrocytes more than unstimulated Ad-hMSCs did (Fig. 3C, right panel and bar graph). To investigate the mechanisms underlying the therapeutic effect of Ad-hMSCs by metformin treatment, bafilomycin A1, which is known as an autophagy inhibitor, was used. Interestingly, the reciprocal regulating effects of metformin-treated Ad-hMSCs on anabolic and catabolic mediators were reversed by bafilomycin A1, indicating that a significant part of Ad-hMSCs optimization by metformin treatment occurs though autophagy induction (Fig. 3D). In contrast, bafilomycin A1 did not affect the gene expression of anabolic and catabolic factors in untreated Ad-hMSCs (Fig. 3D).

Effects of metformin treatment of Ad-hMSCs on pain and cartilage destruction in an OA animal model

The MIA-induced murine model of OA mimics human OA pain and biochemical and structural changes of the disease (31). As pain is the most predominant symptom of OA, we assessed the nociceptive response and histological changes in a rat model of OA. Ad-hMSCs or metformin-stimulated Ad-hMSCs were administered i.v. twice: at 0 and 4 d (Fig. 4A) or 3 and 5 d (Fig. 4B) after OA induction.

In the von Frey hair assessment test, the paw withdrawal latency (PWL) and the paw withdrawal threshold (PWT) were prolonged significantly in the inflamed hind paw of rats given i.v. metformin-stimulated Ad-hMSCs compared with the placebo OA group as well as untreated Ad-hMSC–treated OA group (Fig. 4A, 4B), indicating the superior antinociceptive effects of metformin-treated Ad-hMSCs compared with unstimulated Ad-hMSCs in both groups (Ad-hMSCs treatment at earlier and later dates). Interestingly, the pain-reducing effect of metformin-stimulated Ad-hMSCs was more pronounced in the groups given treatment at the later dates (i.e., 3 and 5 d after OA induction compared with 0 and 4 d) (Fig. 4B versus Fig. 4A). By contrast, unstimulated Ad-hMSCs failed to show pain reduction in OA animals given treatment at both earlier and later dates. These results suggest that metformin-stimulated Ad-hMSCs have superior efficacy in the context of the inflammatory condition, but unstimulated Ad-hMSCs do not.

Next, we determined to evaluate the chondroprotective effect of metformin-stimulated Ad-hMSCs. Isolated knee joints of early

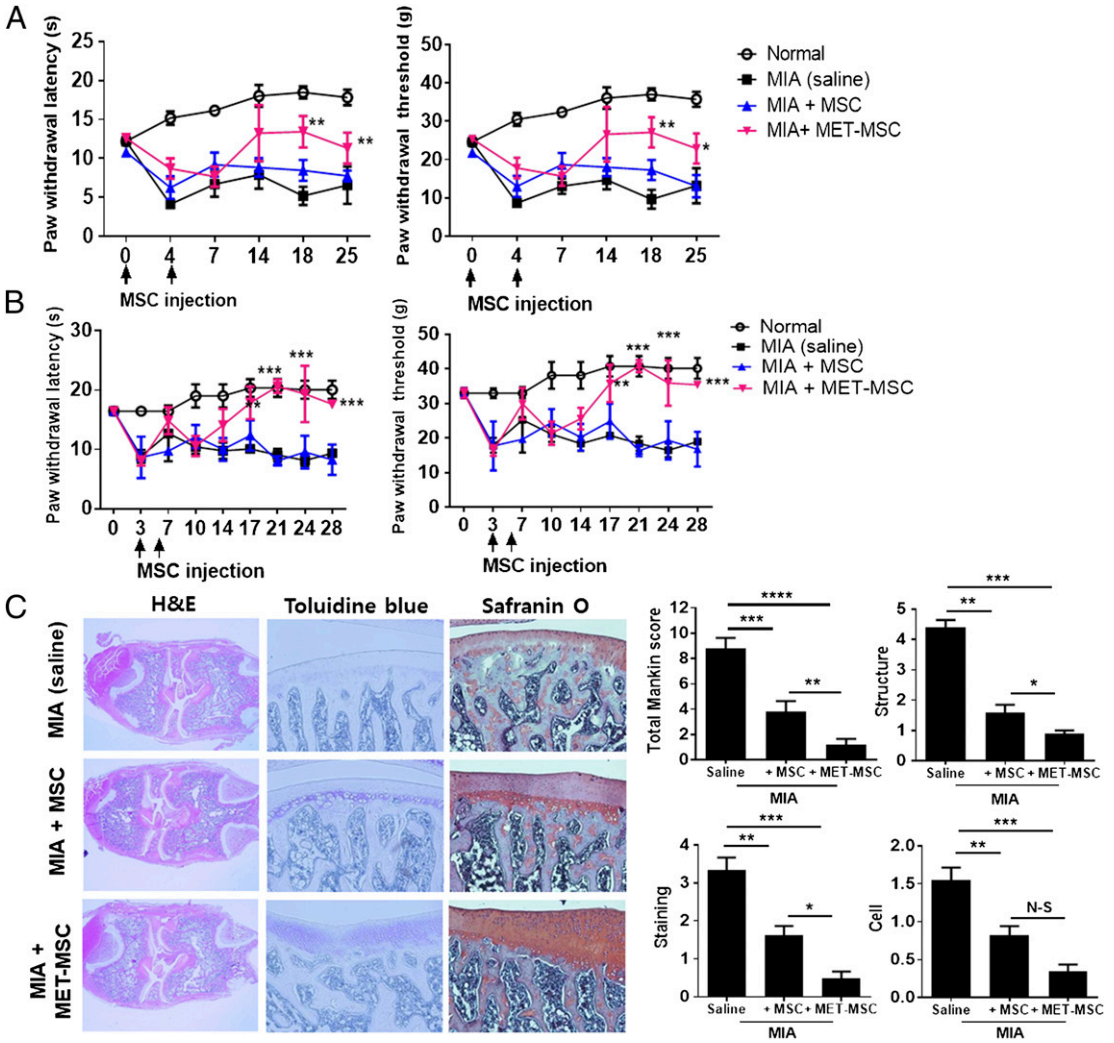

FIGURE 4. Augmented therapeutic effects of metformin-stimulated Ad-hMSCs in a model of MIA-induced OA in rats. OA rats were injected with 3 mg of MIA in the right knee. On days 0 and 4 (**A**) or days 3 and 5 (**B**) after MIA injection, recipient OA rats received i.v. administration of Ad-hMSCs (2×10^6), metformin-stimulated Ad-hMSCs (2×10^6), or saline (control, black square). Behavior tests (PWL and PWT) of mechanical hyperalgesia were evaluated using a dynamic plantar esthesiometer. Combined data from three independent experiments ($n = 12$ per group). The data are expressed as mean ± SD (error bar). (**C**) The knee joints from the OA rats treated with saline (control), unstimulated Ad-hMSCs, or metformin-stimulated Ad-hMSCs (from A) were stained with H&E (original magnification ×20), Safranin O (original magnification ×100), and toluidine blue (original magnification ×100) (left panels). The joint lesions were graded using the modified Mankin scoring system (right panels). Histopathology of the knee joint ($n = 9$ per group); the photographs were taken from one of three independent experiments. $^*p < 0.05$, $^{**}p < 0.01$, $^{***}p < 0.001$.

treatment groups were analyzed microscopically (Fig. 4A). In the control (saline)-treated OA group (upper panel), staining with H&E, toluidine blue, and Safranin O showed joint space narrowing and marked depletion of proteoglycans. These histomorphological changes in the cartilage were attenuated in the Ad-hMSC–treated OA animals. In accordance with the PWL and PWT results, histological assessment also showed superior chondroprotective properties of metformin-stimulated Ad-hMSCs compared with unstimulated Ad-hMSCs (Fig. 4C, left panel). The overall modified Mankin scores were lower in OA rats given metformin-stimulated Ad-hMSCs than in those given unstimulated Ad-hMSCs (Fig. 4C, right panel).

Effects of metformin treatment on Ad-hMSCs in relation to OA pathophysiology

Articular cartilage and the underlying subchondral bone act in concert as a functional unit (32), and the OA disease process affects not only articular cartilage but also entire joints. Subchondral bone remodeling precedes cartilage damage in OA and plays a crucial role in the initiation and progression of the disease and osteophyte formation (33). An increase in subchondral TGF-β expression in response to the abnormal mechanical stress that occurs in OA leads to aberrant bone formation (34). Immunohistochemical analysis revealed inhibited subchondral TGF-β expression in the metformin-treated Ad-hMSCs compared with unstimulated Ad-hMSCs (Fig. 5A).

To assess whether Ad-hMSC treatment can alter pain processing, neurons in the dorsal root ganglion (DRG) at the L4 level were immunostained for CGRP. The number of CGRP-immunoreactive L4 DRG neurons was lower in OA rats injected with unstimulated Ad-hMSCs or metformin-treated Ad-hMSCs compared with the control OA group. And the inhibitory effects on CGRP-expressing neurons in L4 DRG was superior in metformin-stimulated Ad-hMSCs compared with unstimulated cells (Fig. 5B).

Effects of metformin on migration and survival of Ad-hMSCs applied as cell therapy: in vivo imaging

Based on the superior properties of metformin-stimulated Ad-hMSCs, optical in vivo bioluminescence imaging was

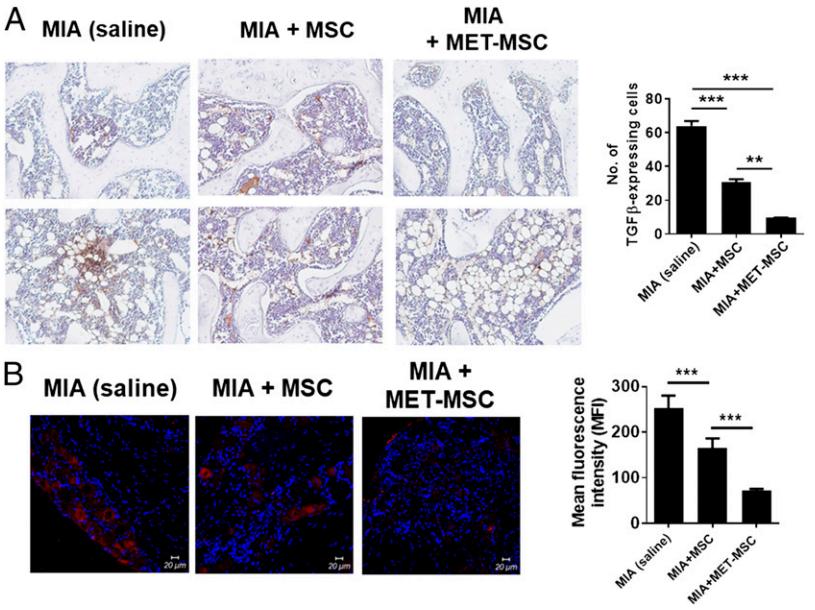

FIGURE 5. Effects of metformin-stimulated Ad-hMSCs on TGF-β expression and pain in an OA animal model. (**A**) Immunohistochemical staining was used to identify the expression of TGF-β in subchondral bone (left panel). Original magnification ×20. The numbers of TGF-β–expressing cells in subchondral bone are presented as means ± SD of three independent experiments (right panel). (**B**) Confocal microscopy of the right L4 DRG shows attenuation of CGRP-reactive neurons in Ad-hMSC–treated OA rats compared with vehicle-treated OA group. Original magnification ×400. $^{**}p < 0.01$, $^{***}p < 0.001$.

used to examine the retention of these cells in the joints. Three days after OA induction by MIA injection, unstimulated Ad-hMSCs or metformin-treated Ad-hMSCs were administered i.v. After the Ad-hMSC injection, in vivo imaging was performed daily (Fig. 6A). More metformin-stimulated Ad-hMSCs were retained in inflamed joints, and they survived for a longer time compared with unstimulated Ad-hMSCs (Fig. 6B).

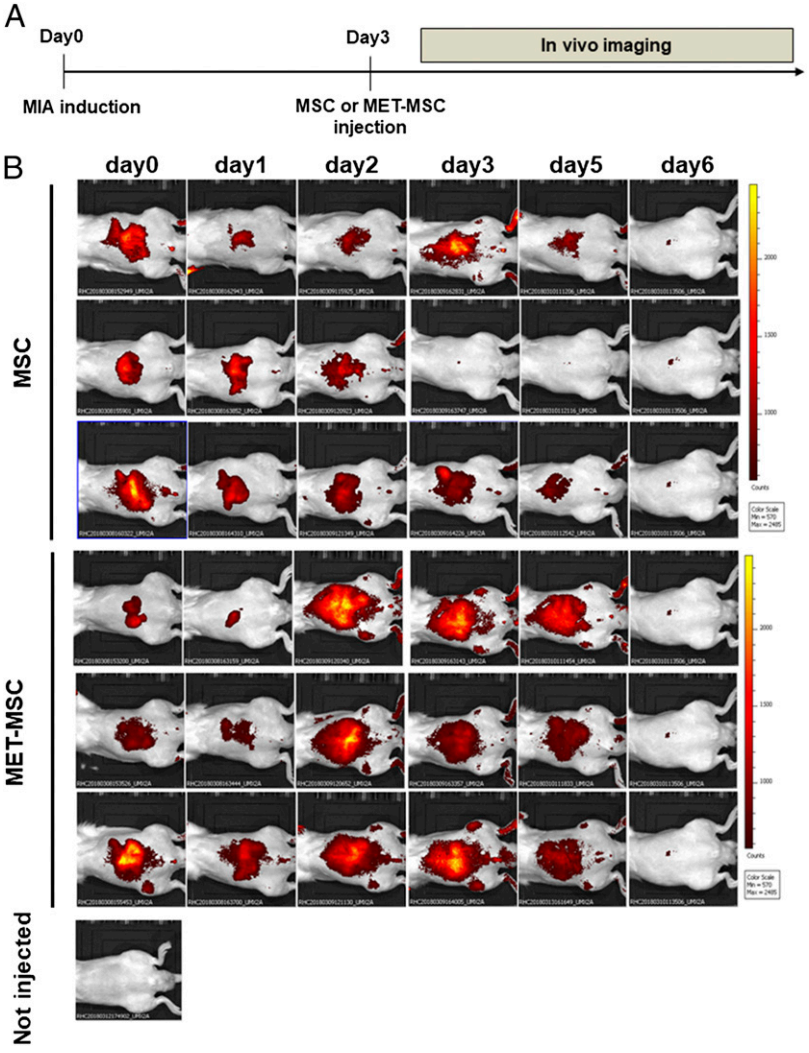

FIGURE 6. Optimized in vivo delivery of metformin-stimulated Ad-hMSCs. (**A**) Schematic diagram depicting the administration of Ad-hMSCs: unstimulated or metformin-stimulated cells. (**B**) In vivo optical bioluminescence imaging demonstrated increased retention and survival of metformin-stimulated Ad-hMSCs compared with unstimulated Ad-hMSCs in MIA-induced OA rats. Data are representative of at least three independent experiments.

Discussion

In this study, we examined the strategy for the use of metformin to augment chondroprotective and pain-reducing properties of Ad-hMSCs as a cell therapy in OA. Metformin treatment in Ad-hMSCs increased the expression of immunoregulatory mediators, including IL-10 and IDO, and inhibited the expression of proinflammatory molecules. Coculture experiments revealed that metformin-treated Ad-hMSCs significantly inhibited catabolic factors and reciprocally induced anabolic factors produced in OA chondrocytes. i.v. administration of metformin-stimulated Ad-hMSCs showed superior chondroprotective and antinociceptive effects in a murine model of OA, whereas untreated Ad-hMSCs failed to show pain-reducing effects. The anti-OA effect of metformin-treated MSCs was associated with inhibited TGFβ expression in subchondral bone and attenuated CGRP-expressing neurons in L4 DRG.

Current therapeutic options of OA include nonsteroidal anti-inflammatory drugs, intra-articular viscosupplementation, and joint replacement in advanced OA patients. Treatment of articular cartilage repair in OA is challenging because the current conservative management of OA may be inadequate to meet the future needs of the aging population. MSCs possess anti-inflammatory and immunosuppressive properties through the secretion of growth factors, cytokines, and chemokines (35). Previous several studies investigating systemic (i.v. or i.p.) MSC administration found that MSCs did not migrate into the joints but localized to the spleen (36–38). Therefore, most, but not all, preclinical and human studies have assessed the therapeutic potential of intra-articular MSC injection, although the results have shown limited efficacy (39–41). By contrast, in our present study, we found that i.v. administration of metformin-treated Ad-hMSCs inhibited articular cartilage damage and showed significant pain-reducing effects. In addition, in vivo imaging showed metformin treatment of Ad-hMSCs augmented their migrating capacity. These results are important for the use of MSCs in clinical practice. Because OA is systemic inflammatory joint disease rather than a "wear-and-tear" degenerative disease, systemic administration of MSCs may be more appropriate than intra-articular injection.

Clinically, many patients with OA show symptoms suggestive of joint inflammation such as morning stiffness, local heat in affected joints, and swelling caused by joint effusion that arises from the synovial proliferation (42). Recent studies have demonstrated that the serum, synovium, and synovial fluids of OA patients have abnormally high levels of proteins, complement components, and proinflammatory cytokines such as IL-1β, IL-6, and HMGB-1 relative to controls (43–45). In our study, metformin treatment significantly suppressed the expression of these inflammatory cytokines in Ad-hMSCs compared with untreated cells; this suggests that metformin has potential in the optimization of Ad-hMSCs as a type of cell therapy for OA.

In conclusion, the current study identified that metformin pretreatment in Ad-hMSCs upregulated their immunoregulatory properties and downregulated their production of proinflammatory and catabolic mediators that are involved in OA pathogenesis but did not affect their MSC characteristics. These effects were associated with autophagy induction in Ad-hMSCs. The metformin-stimulated Ad-hMSCs exhibited more chondroprotective and antinociceptive properties in an experimental OA, whereas unstimulated Ad-hMSCs failed to show significant pain-reducing effects. The augmented antinociceptive effects of metformin-stimulated MSCs in vivo was associated with attenuated number of CGRP-immunoreactive neurons in L4 DRG compared with untreated MSCs-treated OA group. Furthermore, in vivo imaging demonstrated that more metformin-treated MSCs were retained in inflamed joints and they survived for a longer time compared with unstimulated MSCs. Our findings suggest that the immunoregulatory property of metformin may be a simple and innovative strategy to optimize MSCs as a type of cell therapy for OA as well as for other chronic inflammatory diseases.

Acknowledgments

We thank the Institutional Animal Care and Use Committee of the School of Medicine, the Catholic University of Korea, for help in animal care and study.

Disclosures

The authors have no financial conflicts of interest.

References

1. Abramson, S. B., and M. Attur. 2009. Developments in the scientific understanding of osteoarthritis. *Arthritis Res. Ther.* 11: 227.
2. Hashimoto, S., R. L. Ochs, S. Komiya, and M. Lotz. 1998. Linkage of chondrocyte apoptosis and cartilage degradation in human osteoarthritis. *Arthritis Rheum.* 41: 1632–1638.
3. Blanco, F. J., R. Guitian, E. Vázquez-Martul, F. J. de Toro, and F. Galdo. 1998. Osteoarthritis chondrocytes die by apoptosis. A possible pathway for osteoarthritis pathology. *Arthritis Rheum.* 41: 284–289.
4. Sharif, M., A. Whitehouse, P. Sharman, M. Perry, and M. Adams. 2004. Increased apoptosis in human osteoarthritic cartilage corresponds to reduced cell density and expression of caspase-3. *Arthritis Rheum.* 50: 507–515.
5. Robinson, W. H., C. M. Lepus, Q. Wang, H. Raghu, R. Mao, T. M. Lindstrom, and J. Sokolove. 2016. Low-grade inflammation as a key mediator of the pathogenesis of osteoarthritis. *Nat. Rev. Rheumatol.* 12: 580–592.
6. Chadjichristos, C., C. Ghayor, M. Kypriotou, G. Martin, E. Renard, L. Ala-Kokko, G. Suske, B. de Crombrugghe, J. P. Pujol, and P. Galéra. 2003. Sp1 and Sp3 transcription factors mediate interleukin-1 beta down-regulation of human type II collagen gene expression in articular chondrocytes. *J. Biol. Chem.* 278: 39762–39772.
7. Kaneko, S., T. Satoh, J. Chiba, C. Ju, K. Inoue, and J. Kagawa. 2000. Interleukin-6 and interleukin-8 levels in serum and synovial fluid of patients with osteoarthritis. *Cytokines Cell. Mol. Ther.* 6: 71–79.
8. Villiger, P. M., R. Terkeltaub, and M. Lotz. 1992. Monocyte chemoattractant protein-1 (MCP-1) expression in human articular cartilage. Induction by peptide regulatory factors and differential effects of dexamethasone and retinoic acid. *J. Clin. Invest.* 90: 488–496.
9. Kapoor, M., J. Martel-Pelletier, D. Lajeunesse, J. P. Pelletier, and H. Fahmi. 2011. Role of proinflammatory cytokines in the pathophysiology of osteoarthritis. *Nat. Rev. Rheumatol.* 7: 33–42.
10. Attur, M. G., I. R. Patel, R. N. Patel, S. B. Abramson, and A. R. Amin. 1998. Autocrine production of IL-1 beta by human osteoarthritis-affected cartilage and differential regulation of endogenous nitric oxide, IL-6, prostaglandin E2, and IL-8. *Proc. Assoc. Am. Physicians* 110: 65–72.
11. Longobardi, L., L. O'Rear, S. Aakula, B. Johnstone, K. Shimer, A. Chytil, W. A. Horton, H. L. Moses, and A. Spagnoli. 2006. Effect of IGF-I in the chondrogenesis of bone marrow mesenchymal stem cells in the presence or absence of TGF-beta signaling. *J. Bone Miner. Res.* 21: 626–636.
12. Saw, K. Y., A. Anz, C. Siew-Yoke Jee, S. Merican, R. Ching-Soong Ng, S. A. Roohi, and K. Ragavanaidu. 2013. Articular cartilage regeneration with autologous peripheral blood stem cells versus hyaluronic acid: a randomized controlled trial. *Arthroscopy* 29: 684–694.
13. Bieback, K., S. Kern, H. Klüter, and H. Eichler. 2004. Critical parameters for the isolation of mesenchymal stem cells from umbilical cord blood. *Stem Cells* 22: 625–634.
14. Knippenberg, M., M. N. Helder, B. Zandieh Doulabi, P. I. Wuisman, and J. Klein-Nulend. 2006. Osteogenesis versus chondrogenesis by BMP-2 and BMP-7 in adipose stem cells. *Biochem. Biophys. Res. Commun.* 342: 902–908.
15. Hamilton, J. L., M. Nagao, B. R. Levine, D. Chen, B. R. Olsen, and H. J. Im. 2016. Targeting VEGF and its receptors for the treatment of osteoarthritis and associated pain. *J. Bone Miner. Res.* 31: 911–924.
16. Latourte, A., C. Cherifi, J. Maillet, H. K. Ea, W. Bouaziz, T. Funck-Brentano, M. Cohen-Solal, E. Hay, and P. Richette. 2017. Systemic inhibition of IL-6/Stat3 signalling protects against experimental osteoarthritis. *Ann. Rheum. Dis.* 76: 748–755.
17. Zhou, G., R. Myers, Y. Li, Y. Chen, X. Shen, J. Fenyk-Melody, M. Wu, J. Ventre, T. Doebber, N. Fujii, et al. 2001. Role of AMP-activated protein kinase in mechanism of metformin action. *J. Clin. Invest.* 108: 1167–1174.
18. Wang, C., C. Liu, K. Gao, H. Zhao, Z. Zhou, Z. Shen, Y. Guo, Z. Li, T. Yao, and X. Mei. 2016. Metformin preconditioning provide neuroprotection through enhancement of autophagy and suppression of inflammation and apoptosis after spinal cord injury. *Biochem. Biophys. Res. Commun.* 477: 534–540.
19. Zhang, Q., Y. J. Yang, H. Wang, Q. T. Dong, T. J. Wang, H. Y. Qian, and H. Xu. 2012. Autophagy activation: a novel mechanism of atorvastatin to protect

mesenchymal stem cells from hypoxia and serum deprivation via AMP-activated protein kinase/mammalian target of rapamycin pathway. *Stem Cells Dev.* 21: 1321–1332.
20. Altman, R., E. Asch, D. Bloch, G. Bole, D. Borenstein, K. Brandt, W. Christy, T. D. Cooke, R. Greenwald, M. Hochberg, et al. 1986. Development of criteria for the classification and reporting of osteoarthritis. Classification of osteoarthritis of the knee. Diagnostic and Therapeutic Criteria Committee of the American Rheumatism Association. *Arthritis Rheum.* 29: 1039–1049.
21. Jeong, J. H., S. J. Moon, J. Y. Jhun, E. J. Yang, M. L. Cho, and J. K. Min. 2015. Eupatilin exerts antinociceptive and chondroprotective properties in a rat model of osteoarthritis by downregulating oxidative damage and catabolic activity in chondrocytes. *PLoS One* 10: e0130882.
22. Edwards, D. R., G. Murphy, J. J. Reynolds, S. E. Whitham, A. J. Docherty, P. Angel, and J. K. Heath. 1987. Transforming growth factor beta modulates the expression of collagenase and metalloproteinase inhibitor. *EMBO J.* 6: 1899–1904.
23. Kamekura, S., Y. Kawasaki, K. Hoshi, T. Shimoaka, H. Chikuda, Z. Maruyama, T. Komori, S. Sato, S. Takeda, G. Karsenty, et al. 2006. Contribution of runt-related transcription factor 2 to the pathogenesis of osteoarthritis in mice after induction of knee joint instability. *Arthritis Rheum.* 54: 2462–2470.
24. Inada, M., Y. Wang, M. H. Byrne, M. U. Rahman, C. Miyaura, C. López-Otín, and S. M. Krane. 2004. Critical roles for collagenase-3 (Mmp13) in development of growth plate cartilage and in endochondral ossification. *Proc. Natl. Acad. Sci. USA* 101: 17192–17197.
25. Wang, X., P. A. Manner, A. Horner, L. Shum, R. S. Tuan, and G. H. Nuckolls. 2004. Regulation of MMP-13 expression by RUNX2 and FGF2 in osteoarthritic cartilage. *Osteoarthritis Cartilage* 12: 963–973.
26. Higashikawa, A., T. Saito, T. Ikeda, S. Kamekura, N. Kawamura, A. Kan, Y. Oshima, S. Ohba, N. Ogata, K. Takeshita, et al. 2009. Identification of the core element responsive to runt-related transcription factor 2 in the promoter of human type X collagen gene. *Arthritis Rheum.* 60: 166–178.
27. Mistry, D., Y. Oue, M. G. Chambers, M. V. Kayser, and R. M. Mason. 2004. Chondrocyte death during murine osteoarthritis. *Osteoarthritis Cartilage* 12: 131–141.
28. Thomas, C. M., C. J. Fuller, C. E. Whittles, and M. Sharif. 2007. Chondrocyte death by apoptosis is associated with cartilage matrix degradation. *Osteoarthritis Cartilage* 15: 27–34.
29. Hashimoto, S., T. Nishiyama, S. Hayashi, T. Fujishiro, K. Takebe, N. Kanzaki, R. Kuroda, and M. Kurosaka. 2009. Role of p53 in human chondrocyte apoptosis in response to shear strain. *Arthritis Rheum.* 60: 2340–2349.
30. Kim, H. A., Y. J. Lee, S. C. Seong, K. W. Choe, and Y. W. Song. 2000. Apoptotic chondrocyte death in human osteoarthritis. *J. Rheumatol.* 27: 455–462.
31. Kobayashi, K., R. Imaizumi, H. Sumichika, H. Tanaka, M. Goda, A. Fukunari, and H. Komatsu. 2003. Sodium iodoacetate-induced experimental osteoarthritis and associated pain model in rats. *J. Vet. Med. Sci.* 65: 1195–1199.
32. Lories, R. J., and F. P. Luyten. 2011. The bone-cartilage unit in osteoarthritis. *Nat. Rev. Rheumatol.* 7: 43–49.
33. Castañeda, S., J. A. Roman-Blas, R. Largo, and G. Herrero-Beaumont. 2012. Subchondral bone as a key target for osteoarthritis treatment. *Biochem. Pharmacol.* 83: 315–323.
34. Zhen, G., C. Wen, X. Jia, Y. Li, J. L. Crane, S. C. Mears, F. B. Askin, F. J. Frassica, W. Chang, J. Yao, et al. 2013. Inhibition of TGF-β signaling in mesenchymal stem cells of subchondral bone attenuates osteoarthritis. *Nat. Med.* 19: 704–712.
35. Caplan, A. I. 2007. Adult mesenchymal stem cells for tissue engineering versus regenerative medicine. *J. Cell. Physiol.* 213: 341–347.
36. Mao, F., W. R. Xu, H. Qian, W. Zhu, Y. M. Yan, Q. X. Shao, and H. X. Xu. 2010. Immunosuppressive effects of mesenchymal stem cells in collagen-induced mouse arthritis. *Inflamm. Res.* 59: 219–225.
37. Choi, J. J., S. A. Yoo, S. J. Park, Y. J. Kang, W. U. Kim, I. H. Oh, and C. S. Cho. 2008. Mesenchymal stem cells overexpressing interleukin-10 attenuate collagen-induced arthritis in mice. *Clin. Exp. Immunol.* 153: 269–276.
38. González, M. A., E. Gonzalez-Rey, L. Rico, D. Büscher, and M. Delgado. 2009. Treatment of experimental arthritis by inducing immune tolerance with human adipose-derived mesenchymal stem cells. *Arthritis Rheum.* 60: 1006–1019.
39. Murphy, J. M., D. J. Fink, E. B. Hunziker, and F. P. Barry. 2003. Stem cell therapy in a caprine model of osteoarthritis. *Arthritis Rheum.* 48: 3464–3474.
40. Davatchi, F., B. S. Abdollahi, M. Mohyeddin, F. Shahram, and B. Nikbin. 2011. Mesenchymal stem cell therapy for knee osteoarthritis. Preliminary report of four patients. *Int. J. Rheum. Dis.* 14: 211–215.
41. Farrell, E., N. Fahy, A. E. Ryan, C. O. Flatharta, L. O'Flynn, T. Ritter, and J. M. Murphy. 2016. vIL-10-overexpressing human MSCs modulate naïve and activated T lymphocytes following induction of collagenase-induced osteoarthritis. *Stem Cell Res. Ther.* 7: 74.
42. Sellam, J., and F. Berenbaum. 2010. The role of synovitis in pathophysiology and clinical symptoms of osteoarthritis. *Nat. Rev. Rheumatol.* 6: 625–635.
43. Sohn, D. H., J. Sokolove, O. Sharpe, J. C. Erhart, P. E. Chandra, L. J. Lahey, T. M. Lindstrom, I. Hwang, K. A. Boyer, T. P. Andriacchi, and W. H. Robinson. 2012. Plasma proteins present in osteoarthritic synovial fluid can stimulate cytokine production via toll-like receptor 4. *Arthritis Res. Ther.* 14: R7.
44. Gobezie, R., A. Kho, B. Krastins, D. A. Sarracino, T. S. Thornhill, M. Chase, P. J. Millett, and D. M. Lee. 2007. High abundance synovial fluid proteome: distinct profiles in health and osteoarthritis. *Arthritis Res. Ther.* 9: R36.
45. Ke, X., G. Jin, Y. Yang, X. Cao, R. Fang, X. Feng, and B. Lei. 2015. Synovial fluid HMGB-1 levels are associated with osteoarthritis severity. *Clin. Lab.* 61: 809–818.